

Two-loop corrections in power spectrum in models of inflation with PBHs formation

Hassan Firouzjahi*

*School of Astronomy, Institute for Research in Fundamental Sciences (IPM)
P. O. Box 19395-5746, Tehran, Iran*

Abstract

We calculate the two-loop corrections in curvature perturbation power spectrum in models of single field inflation incorporating an intermediate USR phase employed for PBHs formation. Among the total eleven one-particle irreducible Feynman diagrams, we calculate the corrections from the “double scoop” two-loop diagram involving two vertices of quartic Hamiltonians. We demonstrate that the fractional two-loop correction in power spectrum scales like the square of the fractional one-loop correction. We confirm our previous findings that the loop corrections become arbitrarily large when the transition from the USR phase to the final attractor phase is very sharp. This suggests that in order for the analysis to be under perturbative control against the loop corrections, one requires a mild transition with a long enough relaxation period towards the final attractor phase.

*firouz@ipm.ir

1 Introduction

There have been intense debates in recent literature on the nature of loop corrections in models of single field inflation involving an intermediate phase of ultra slow-roll (USR) inflation [1–36], for earlier works on loop corrections in power spectrum during inflation see for example [37–41]. These models have been employed to generate primordial black holes (PBHs) as candidates for the observed dark matter [42–45], for a review see [46–50]. During the USR phase of inflation with a flat potential, the curvature perturbation power spectrum grows on superhorizon scales. The enhancement in power spectrum allows one to use this setup to generate PBHs on desired scales. However, the rapid growth of the power spectrum during the intermediate USR phase may cause troubles. More specifically, it was argued in [1] that the one-loop corrections induced from small scales USR modes can affect the long CMB scale perturbations. Correspondingly, it was argued originally in [1] that the analysis is not under perturbative control and the setup is not trusted for PBHs formation. Following [1], the question of one-loop corrections in power spectrum in these models was studied with different (conflicting) conclusions. For example, the conclusion in [1] was criticized in [3,4] where it was argued that the one-loop corrections can be harmless if the transition to the final attractor phase is smooth enough. Similarly, in [13], employing δN formalism, it was argued that the one-loop corrections in models with a mild transition are suppressed by the slow-roll parameters and the setup is reliable for PBHs formations. This question was also studied numerically in [27] and using the separate universe formalism in [28].

In order to calculate the total one-loop corrections in power spectrum, one needs to include both the cubic and quartic interactions. The cubic interactions were calculated originally by Maldacena [51] but there is no concrete result for the full quartic interaction including the USR phase, but for earlier studies on quartic action see [52,53]. In [11], we have employed the formalism of effective field theory (EFT) of inflation which enabled us to calculate the cubic and the quartic Hamiltonians in reasonable ease in the decoupling limit. Furthermore, we were able to incorporate the effects of the sharpness of the transition from the intermediate USR phase to the final attractor phase as well. It was shown in [11] that one-loop corrections can be dangerous in models with a sharp transition, supporting the conclusion of [1].

Based on the physical intuitions and the notion of decoupling of scales, it looks counterintuitive as how the small scales can affect the long modes in the first place [4,25]. Motivated by this question, the effect of loop corrections was critically revisited in [23] and [24] where it was claimed that the one-loop correction cancel in the setup of interest. Specifically, in [23] the contributions of the boundary terms were highlighted which were not incorporated in previous works. On the other hand, in [24] it was argued that the large loop corrections are cancelled once the UV limit of the momentum is taken by some $i\epsilon$ prescription. In both [23,24], like many other previous works, only the cubic interactions were considered. The conclusions of [23,24] were reviewed critically in [25] highlighting the flaws in their arguments. More recently, there were new claims of loop cancellation in [54–56], we would like to come back to the results of these claims elsewhere.

As for the physical origins of the loop corrections, the basic idea is that the non-linear coupling between the long and short modes induces a source term for the evolution of the long mode. At the same time, the long mode modulates the spectrum of the short modes. This modulation becomes significant if the power spectrum of the short modes is highly scale-dependent such as in the USR setup. The combined effects of the non-linear coupling between the long and short modes and the

modulation of the short modes by the long mode back-reacts on the long mode itself, causing the one-loop correction [3, 15, 25].

Motivated by the above discussions, in this work we aim to calculate the corrections in power spectrum at the two-loop order. As one may expect, the analysis at two-loop order are significantly more complicated than in one-loop case. First, we have more Feynman diagrams involving not only the cubic and quartic interactions, but also the quintic and sextic Hamiltonians. Secondly, most of these Feynman diagrams involve double or higher order nested in-in integrals which make the time integral very complicated. As we shall see, there are in total eleven one-particle irreducible Feynman diagrams at two-loop level. Out of these eleven diagrams, we consider the case of the “double scoop” digram which involves a double nested time integral containing two quartic Hamiltonians. We believe that the results from this case are illustrative enough which can shed light on the structure of the two-loop corrections.

2 The Setup

In this section we briefly review our setup. This is the same setup as employed in [1], a single field model of inflation containing three stages, $SR \rightarrow USR \rightarrow SR$, where the first and the third stages are SR phases while the intermediate stage is a USR phase. The long CMB scale perturbations leave the horizon during the first stage with an amplitude of curvature perturbation fixed by the COBE normalization. The second phase is tuned to generate the PBHs at the desired scale as the seed of dark matter. Typically, the intermediate USR phase may start at around 30 e-folds after the long CMB modes have left the horizon and it lasts for about 2-3 e-folds. Finally, the USR phase is followed by the third SR phase during which the system reaches its final attractor phase.

During the SR phases the curvature perturbation \mathcal{R} is frozen on superhorizon scales. However, during the USR phase it experiences an exponential growth [57–63]. The rapid growth of the modes which leave the horizon during the USR phase is the key idea behind the enhancement in curvature perturbation power spectrum to generate PBHs on the corresponding scales. In addition, the superhorizon growth of curvature perturbation is the key behind the violation of the Maldacena non-Gaussianity consistency condition in USR setup [58–60, 64–76].

Starting with the FLRW metric,

$$ds^2 = -dt^2 + a(t)^2 d\mathbf{x}^2, \quad (1)$$

the background fields equations for the inflaton field ϕ and the scale factor $a(t)$ during the USR phase are given by,

$$\ddot{\phi}(t) + 3H\dot{\phi}(t) = 0, \quad 3M_P^2 H^2 \simeq V_0, \quad (2)$$

in which M_P is the reduced Planck mass, H is the Hubble expansion rate during inflation and V_0 is the potential during the USR phase.

Since H is very nearly constant during the USR phase then $\dot{\phi} \propto a^{-3}$. Correspondingly, the first slow-roll parameter $\epsilon \equiv -\frac{\dot{H}}{H^2}$ falls off like a^{-6} while the second slow-roll parameter $\eta \equiv \frac{\dot{\epsilon}}{H\epsilon}$ is nearly constant, $\eta \simeq -6$. It is assumed that the USR phase is extended between the interval $\tau_s < \tau < \tau_e$ so ϵ at the end of USR phase is given by $\epsilon_e = \epsilon_i \left(\frac{\tau_e}{\tau_s}\right)^6$ in which ϵ_i is the initial value of ϵ during the first SR phase. Here τ is the conformal time, related to cosmic time via $d\tau = dt/a(t)$ with the

understanding that towards the end of inflation $\tau \rightarrow 0$. Alternatively, working with the number of e-fold $dN = Hdt$ as the clock, the duration of the USR phase is given by $\Delta N \equiv N(\tau_e) - N(\tau_s)$ yielding to $\epsilon_e = \epsilon_i e^{-6\Delta N}$. For PBHs formation we typically require ΔN to be around 2 to 3 e-folds.

To simplify the analysis, we assume the transitions $SR \rightarrow USR$ and $USR \rightarrow SR$ happen instantaneously, at $\tau = \tau_s$ and $\tau = \tau_e$ respectively. However, it may take time to end up in its attractor phase during the final SR phase. This is determined by the sharpness (actually the relaxation) parameter h initially defined in [76] via

$$h = -6\sqrt{\frac{\epsilon_V}{\epsilon_e}}, \quad (3)$$

in which ϵ_V is the value of the slow-roll parameter during the final attractor phase which is determined as usual by the first derivative of the potential. Note that by construction $h < 0$. In our analysis, we assume a sharp enough transition so $|h| > 1$. For mild transition, say h at the order of slow-roll parameters, the mode function keeps evolving during the final phase and the analysis become complicated. However, for a sharp transition, the system reaches the attractor phase quickly and the errors in our analytical results are expected to be negligible.

For a very sharp transition with $h \rightarrow -\infty$, ϵ evolves rapidly to a larger value such that ϵ at the end of inflation is given by $\epsilon(\tau_0) \simeq \epsilon_V = \epsilon_e (\frac{h}{6})^2$. On the other hand, for an ‘‘instant’’ sharp transition which was assumed in [1, 2], one has $h = -6$. In this case ϵ in the final SR phase is frozen to its value at the end of USR phase, i.e. $\epsilon_V = \epsilon_e$.

The evolution of the slow-roll parameters after the USR phase are studied in [76]. In particular, ϵ is smooth across the transition point but η has a jump at $\tau = \tau_e$. Prior to the transition and near the end of USR phase, $\eta = -6$ while right after the transition $\eta = -6 - h$. Following [76], we can approximate η near the transition point as follows,

$$\eta = -6 - h\theta(\tau - \tau_e) \quad \tau_e^- < \tau < \tau_e^+, \quad (4)$$

yielding to

$$\frac{d\eta}{d\tau} = -h\delta(\tau - \tau_e), \quad \tau_e^- < \tau < \tau_e^+. \quad (5)$$

As we shall see, the jump in η highlighted by the Dirac delta function above, plays crucial role in the loop corrections.

After presenting our background, we briefly review the perturbations in this setup. To perform the in-in formalism we need the mode function for the comoving curvature perturbation \mathcal{R} during the USR and the follow up SR phase. In the Fourier space, the mode function is given by,

$$\mathcal{R}(\mathbf{x}, t) = \int \frac{d^3k}{(2\pi)^3} e^{i\mathbf{k}\cdot\mathbf{x}} \hat{\mathcal{R}}_{\mathbf{k}}(t), \quad (6)$$

where, as usual, the operator $\hat{\mathcal{R}}_{\mathbf{k}}(t)$ is expressed in terms of the creation and annihilation operators via $\hat{\mathcal{R}}_{\mathbf{k}}(t) = \mathcal{R}_k(t)a_{\mathbf{k}} + \mathcal{R}_k^*(t)a_{-\mathbf{k}}^\dagger$. In this notation, $\hat{\mathcal{R}}_{\mathbf{k}}$ is a quantum operator while \mathcal{R}_k is the usual mode function. The creation and annihilation operators satisfy the standard commutation relations $[a_{\mathbf{k}}, a_{\mathbf{k}'}^\dagger] = (2\pi)^3 \delta(\mathbf{k} - \mathbf{k}')$.

The quantum initial condition is fixed by the Bunch-Davies vacuum with the mode function,

$$\mathcal{R}_k^{(1)} = \frac{H}{M_P \sqrt{4\epsilon_i k^3}} (1 + ik\tau) e^{-ik\tau}, \quad (\tau < \tau_s). \quad (7)$$

During the intermediate USR phase, the mode function is parameterized via,

$$\mathcal{R}_k^{(2)} = \frac{H}{M_P \sqrt{4\epsilon_i k^3}} \left(\frac{\tau_s}{\tau} \right)^3 \left[\alpha_k^{(2)} (1 + ik\tau) e^{-ik\tau} + \beta_k^{(2)} (1 - ik\tau) e^{ik\tau} \right], \quad (8)$$

in which the coefficients $\alpha_k^{(2)}$ and $\beta_k^{(2)}$ are fixed by imposing the continuity of the mode function and its time derivative, yielding

$$\alpha_k^{(2)} = 1 + \frac{3i}{2k^3 \tau_s^3} (1 + k^2 \tau_s^2), \quad \beta_k^{(2)} = -\frac{3i}{2k^3 \tau_s^3} (1 + ik\tau_s)^2 e^{-2ik\tau_s}. \quad (9)$$

Finally, imposing the matching conditions at τ_e , the outgoing mode function during the final SR phase is obtained to be [11],

$$\mathcal{R}_k^{(3)} = \frac{H}{M_P \sqrt{4\epsilon(\tau) k^3}} \left[\alpha_k^{(3)} (1 + ik\tau) e^{-ik\tau} + \beta_k^{(3)} (1 - ik\tau) e^{ik\tau} \right], \quad (10)$$

in which the coefficients $\alpha_k^{(3)}$ and $\beta_k^{(3)}$ are determined to be,

$$\alpha_k^{(3)} = \frac{1}{8k^6 \tau_s^3 \tau_e^3} \left[3h(1 - ik\tau_e)^2 (1 + ik\tau_s)^2 e^{2ik(\tau_e - \tau_s)} - i(2k^3 \tau_s^3 + 3ik^2 \tau_s^2 + 3i)(4ik^3 \tau_e^3 - hk^2 \tau_e^2 - h) \right],$$

and

$$\beta_k^{(3)} = \frac{-1}{8k^6 \tau_s^3 \tau_e^3} \left[3(1 + ik\tau_s)^2 (h + hk^2 \tau_e^2 + 4ik^3 \tau_e^3) e^{-2ik\tau_s} + ih(1 + ik\tau_e)^2 (3i + 3ik^2 \tau_s^2 + 2k^3 \tau_s^3) e^{-2ik\tau_e} \right].$$

With the mode functions given above, we can calculate the loop corrections in curvature perturbations power spectrum. To fix the notation, the momentum for the long CMB modes are denoted by \mathbf{p}_1 and \mathbf{p}_2 while the momentum associated to the short modes which run inside the loops are denoted by \mathbf{q} and \mathbf{k} . There is the vast hierarchy $p_i \ll q, k$. In our analysis, we are interested in the loop corrections induced from the modes which leave the horizon during the USR phase. Therefore, we cut the loop integrals in the intervals $q_s \leq q < q_e$ in which $q_s = -\frac{1}{\tau_s}$ and $q_e = -\frac{1}{\tau_e}$ are the modes which leave the horizon at the start and at the end of USR phase respectively. Furthermore, the duration of the USR period $\Delta N \equiv N(\tau_e) - N(\tau_s)$ is related to q_s and q_e via

$$e^{-\Delta N} = \frac{\tau_e}{\tau_s} = \frac{q_s}{q_e}. \quad (11)$$

As mentioned previously, to have PBHs formation with the desired properties, we typically require $\Delta N \sim 2 - 3$.

Before closing this review, there is an important comment in order. In our setup, to simplify the analysis, we consider an instant transition at $\tau = \tau_e$ to the final SR phase. However, the mode functions may keep evolving after the transition until it reaches its attractor value. This is controlled by the sharpness (relaxation) parameter h . For example, for an instant sharp transition with $h = -6$ which was studied in [1, 2], the final value of \mathcal{R} at the end of inflation is smaller by a factor of 1/4 compared to its value at the end of USR. This is because the mode function is not frozen right after the transition and it keeps evolving until it reaches its attractor value. However, for a very sharp transition with $h \rightarrow -\infty$, the mode function freezes immediately after the USR phase. This is the limit which was studied in [58, 60] which yields to $f_{NL} = \frac{5}{2}$. But, as shown in [76], for a mild

transition with $|h| \ll 1$, most of non-Gaussianity is washed out during the subsequent evolution of SR phase. With the above discussions in mind, one should distinguish between an instant transition and a sharp transition. For example, one can relax the assumption of an instant transition and assume the transition to takes place within some time interval [15,27]. However, this will complicate the theoretical analysis which is beyond the scope of our current work.

3 Two-loops Feynman Diagrams and Interaction Hamiltonians

To calculate the loop corrections in curvature perturbation power spectrum $\mathcal{P}_{\mathcal{R}}$, we need the interaction Hamiltonians. Here we present the structure of two-loops Feynman diagrams and the subset of interaction Hamiltonians necessary for our two-loop calculations.

To understand the structure of Feynman diagrams associated at two-loop level, consider a general n -loop, one-particle irreducible Feynman diagram associated to the following scalar type potential

$$V = \sum_n g_n \phi^n \quad (n > 2), \quad (12)$$

in which g_n is the coupling (vertex) and n is the order of interaction. For example, for the cubic and quartic interactions we have $n = 3$ and $n = 4$ respectively. Suppose we have a Feynman diagram with L loops, P internal propagators, V_n vertices associated to each power of interaction n and N external lines. For example, in our case of interest, $L = 2$ (two-loops) and $N = 2$ (two external lines for power spectrum). Then using the following topological conditions [82],

$$L = P - \sum_n V_n + 1 \quad (13)$$

and

$$N + 2P = \sum_n nV_n, \quad (14)$$

we obtain the following relation between L , N and V_n ,

$$2L = (2 - N) + \sum_n (n - 2)V_n. \quad (15)$$

For the loop corrections in power spectrum with $N = 2$, this further simplifies to

$$2L = \sum_n (n - 2)V_n \quad (N = 2). \quad (16)$$

In particular, for one-loop corrections, the above condition allows only two Feynman diagrams, a single quartic vertex and a diagram with two cubic vertices as studied in details in [11].

Now in our current case of interest with two-loop corrections ($L = 2$), Eq. (16) yields the following constraint,

$$4 = V_3 + 2V_4 + 3V_5 + 4V_6. \quad (17)$$

Based on the allowed integer solutions of the above equation, one obtains the allowed Feynman diagrams. Here are all possible allowed solutions,

$$\begin{aligned}
(1) & : V_6 = V_5 = V_3 = 0, V_4 = 2, \\
(2) & : V_6 = V_5 = V_4 = 0, V_3 = 4, \\
(3) & : V_6 = V_5 = 0, V_4 = 1, V_3 = 2, \\
(4) & : V_6 = V_4 = 0, V_3 = V_5 = 1, \\
(5) & : V_3 = V_4 = V_5 = 0, V_6 = 1.
\end{aligned} \tag{18}$$

The above solutions yield to 11 distinct two-loop diagrams as plotted in Fig. 1. The Feynman diagrams in the first category involves two vertices of quartic Hamiltonian \mathbf{H}_4 (diagrams (a) and (b) in Fig. 1), while the diagrams in the second category involve four vertices of the cubic Hamiltonian \mathbf{H}_3 (diagrams (c) and (d)). The diagrams in the third category contain three vertices, one from \mathbf{H}_4 and two from \mathbf{H}_3 (diagrams (e), (f), (g) and (h)). On the other hand, the diagram in the fourth category involves two vertices, one from \mathbf{H}_3 and one from the quintic interaction \mathbf{H}_5 (diagrams (k) and (l)). Finally, the diagram in the fifth category involves a single vertex from the sextic Hamiltonian \mathbf{H}_6 , (diagram (m)). From the above discussions we see that we need $\mathbf{H}_3, \mathbf{H}_4, \mathbf{H}_5$ and \mathbf{H}_6 to calculate the full two-loop corrections in $\mathcal{P}_{\mathcal{R}}$.

The cubic action for the curvature perturbations \mathcal{R} and the corresponding cubic Hamiltonian was calculated in details by Maldacena [51]. However, calculating the quartic action and the corresponding quartic Hamiltonian in this method is a very difficult task. Fortunately, the formalism of EFT of inflation [77, 78] provides a very useful alternative in which the interaction Hamiltonians can be calculated with reasonable ease. In particular, in the decoupling limit where the gravitational backreactions are neglected, the EFT formalism was employed to calculate the cubic and quartic Hamiltonians in [11] (see also [65] for the first work on this direction, calculating the cubic Hamiltonian). While the cubic and the quartic Hamiltonians were constructed in [11], one still needs to calculate \mathbf{H}_5 and \mathbf{H}_6 to perform the full two-loop corrections. In principle, it is possible to calculate \mathbf{H}_5 and \mathbf{H}_6 using the EFT approach, but it turns out that there are new technical complications which require careful considerations [83].

The analysis of full two-loop corrections associated to the above 11 diagrams are a demanding task. As a first step forward, we calculate the two-loop corrections from the ‘‘double scoop’’ diagram (a) which is somewhat easier to handle technically. This is because this diagram involves two vertices so one deals with double nested in-in integrals (this is also true for diagram (b)). However, diagrams (c), (d), (e), (f), (g) and (h) contain nested integrals with three-fold or four-fold time integrals involving \mathbf{H}_3 or \mathbf{H}_4 which are far more complicated than diagram (a). As we shall see, the analysis even for the simple-looking diagram (a) is non-trivial. Having said this, physically one expects that the result obtained from this single diagram shed lights on the structure of two-loop corrections which should not be vary different than the remaining diagrams.

Here we briefly review the results of [11] which are required to calculate the quartic Hamiltonian to calculate the loop corrections from diagram (a). We refer the reader to [11] for further details.

The quadratic action employed to quantize the free theory is given by

$$S_2 = M_P^2 \int d\tau d^3x a^2 \epsilon H^2 (\pi'^2 - (\partial_i \pi)^2), \tag{19}$$

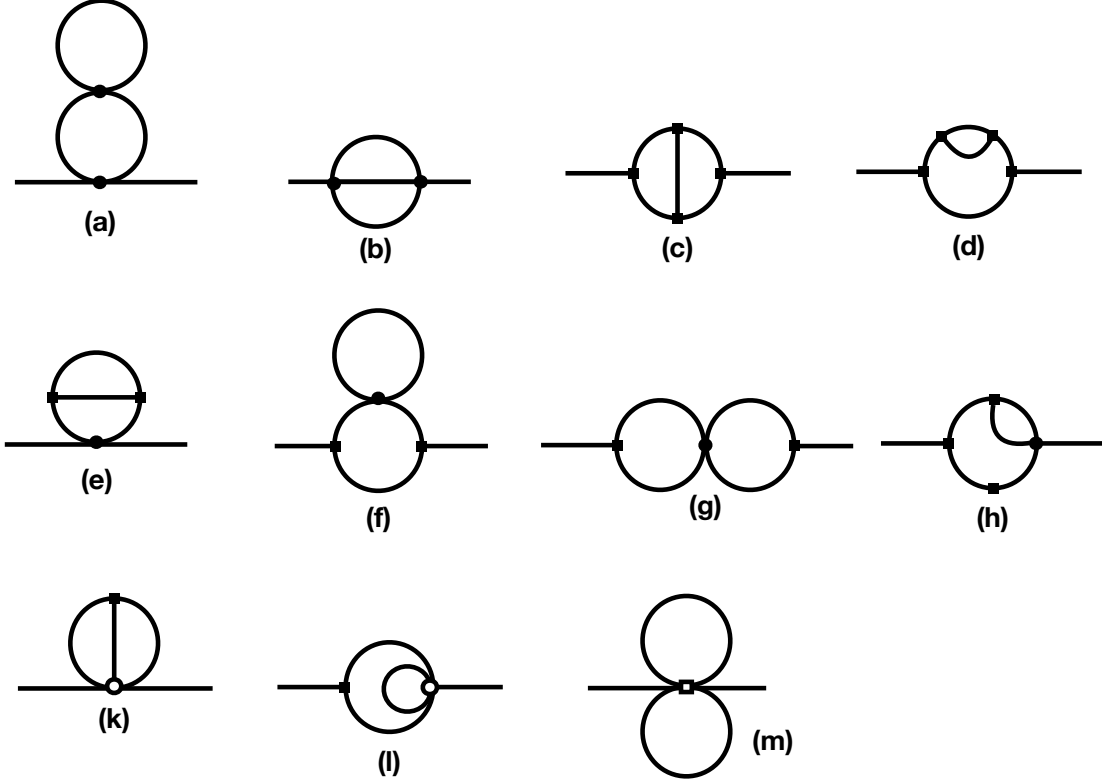


Figure 1: The one-particle irreducible Feynman diagrams for the two-loop corrections constructed from the solutions of Eq. (18). The diagrams (a) and (b) belong to category (1) in Eq. (18), diagrams (c) and (d) to category (2), diagrams (e), (f), (g) and (h) to category (3), diagrams (k) and (l) belong to categories (4) while diagram (m) belongs to category (5).

in which a prime denotes the derivative with respect to the conformal time. Here $\pi(x^\mu)$ is the Goldstone boson associated to time diffeomorphism breaking which is related to curvature perturbations \mathcal{R} [77, 78].

The cubic action is given by,

$$S_{\pi^3} = M_P^2 H^3 \int d\tau d^3x \eta \epsilon a^2 \left[\pi \pi'^2 - \pi (\partial\pi)^2 \right], \quad (20)$$

and the corresponding cubic interaction Hamiltonian is obtained to be [65],

$$\mathbf{H}_3 = -M_P^2 H^3 \eta \epsilon a^2 \int d^3x \left[\pi \pi'^2 + \frac{1}{2} \pi^2 \partial^2 \pi \right]. \quad (21)$$

On the other hand, the quartic action is obtained to be,

$$S_{\pi^4} = \frac{M_P^2}{2} \int d\tau d^3x \epsilon a H^3 (\eta^2 a H + \eta') \left[\pi^2 \pi'^2 - \pi^2 (\partial\pi)^2 \right]. \quad (22)$$

In particular, note that there is the term η' which induces a delta contribution in the interaction Hamiltonian when η undergoes a jump from the USR phase to the final SR phase as given by Eq. (5).

As observed in [11], when calculating the quartic Hamiltonian, one has to be careful as the time derivative interaction $\pi' \pi^2$ in \mathbf{H}_3 induces a new term in the quartic Hamiltonian [80, 81]. As a result,

one can not simply conclude that $\mathbf{H}_4 = -\mathbf{L}_4$. More specifically, the quartic Hamiltonian receives additional contribution $+M_P^2 H^4 \eta^2 \epsilon a^2 \pi^2 \pi'^2$ from the cubic action. Combining all contributions, the total quartic Hamiltonian is obtained to be [11]

$$\mathbf{H}_4 = \frac{M_P^2}{2} \epsilon a H^3 \int d^3x \left[(\eta^2 a H - \eta') \pi^2 \pi'^2 + (\eta^2 a H + \eta') \pi^2 (\partial\pi)^2 \right]. \quad (23)$$

The interaction Hamiltonians (21) and (23) have been used in [11] to calculate the one-loop corrections to power spectrum.

We are interested in curvature perturbation on comoving surface \mathcal{R} while the above interaction Hamiltonians are written in terms of the Goldstone field π . The relation between \mathcal{R} and π is non-linear. For example, to cubic order in π , they are related to each other via [52, 53],

$$\begin{aligned} \mathcal{R} &= -H\pi + \left(H\pi\dot{\pi} + \frac{\dot{H}}{2}\pi^2 \right) + \left(-H\pi\dot{\pi}^2 - \frac{H}{2}\ddot{\pi}\pi^2 - \dot{H}\dot{\pi}\pi^2 - \frac{\ddot{H}}{6}\pi^3 \right), \\ &= -H\pi + \frac{1}{2} \frac{d}{dt} (H\pi^2) - \frac{1}{6} \frac{d^2}{dt^2} (H\pi^3). \end{aligned} \quad (24)$$

However, we calculate the loop corrections in power spectrum at the end of inflation $\tau = \tau_0 \rightarrow 0$ when the system is in the slow-roll regime and the long mode perturbations are frozen, $\dot{\pi} = \ddot{\pi} = 0$. Fortunately, in this limit one can neglect the non-linear corrections in \mathcal{R} in Eq. (24) and simply assume the linear relation between \mathcal{R} and π ,

$$\mathcal{R} = -H\pi, \quad (\tau \rightarrow \tau_0). \quad (25)$$

Because of this linear relation between π and \mathcal{R} , we can use π and \mathcal{R} interchangeably in the following in-in integrals. More specifically, we will use the mode function of \mathcal{R} from the free theory (in the interaction picture) in place of the π perturbations in the following in-in integrals.

4 Loop Corrections in Power Spectrum

To calculate the loop corrections in power spectrum we use the perturbative in-in formalism [79]. The expectation value of the quantum operator $\hat{O}[\tau_0]$ at the end of inflation τ_0 is given by,

$$\langle \hat{O}(\tau_0) \rangle = \left\langle \left[\bar{\mathbb{T}} \exp \left(i \int_{-\infty}^{\tau_0} d\tau' H_{\text{in}}(\tau') \right) \right] \hat{O}(\tau_0) \left[\mathbb{T} \exp \left(-i \int_{-\infty}^{\tau_0} d\tau' H_{\text{in}}(\tau') \right) \right] \right\rangle, \quad (26)$$

in which, as usual, \mathbb{T} and $\bar{\mathbb{T}}$ represent the time ordering and anti-time ordering respectively while $H_{\text{in}}(t)$ is the interaction Hamiltonian. In our case $\hat{O}(\tau_0) = \mathcal{R}_{\mathbf{p}_1}(\tau_0) \mathcal{R}_{\mathbf{p}_2}(\tau_0)$, while for the Feynman diagram (a) which we consider here, we only need the quartic interactions so $H_{\text{in}} = \mathbf{H}_4$.

To calculate the two-loop corrections, we need to expand the in-in formula Eq. (26) to second order in powers of H_{in} . For this purpose, it turns out to be more convenient to employ the Weinberg method of the commutator series associated to equation (26). To second order in interaction, this yields [79],

$$\langle \hat{O}(\tau_0) \rangle = i^2 \int_{-\infty}^{\tau_0} d\tau_2 \int_{-\infty}^{\tau_2} d\tau_1 \left\langle \left[H_{\text{in}}(\tau_1), [H_{\text{in}}(\tau_2), \hat{O}(\tau_0)] \right] \right\rangle \quad (27)$$

$$= 2 \int_{-\infty}^{\tau_0} d\tau_2 \int_{-\infty}^{\tau_2} d\tau_1 \text{Re} \left[\langle \mathbf{H}_4(\tau_1) \hat{O}(\tau_0) \mathbf{H}_4(\tau_2) \rangle - \langle \mathbf{H}_4(\tau_1) \mathbf{H}_4(\tau_2) \hat{O}(\tau_0) \rangle \right], \quad (28)$$

with $\hat{O}(\tau_0) \equiv \mathcal{R}_{\mathbf{p}_1}(\tau_0)\mathcal{R}_{\mathbf{p}_2}(\tau_0)$.

Depending on the contractions of external leg operators $\hat{O}(\tau_0)$, there are two distinct Feynman diagrams as shown by diagram (a) and (b) in Fig. 1. The digram (a) corresponds to the situation in which $\hat{O}(\tau_0)$ contracts only with $\mathbf{H}_4(\tau_2)$, with no contractions to $\mathbf{H}_4(\tau_1)$. On the other hand, the diagram (b) corresponds to the case where $\hat{O}(\tau_0)$ contracts jointly with both $\mathbf{H}_4(\tau_2)$ and $\mathbf{H}_4(\tau_1)$. As mentioned before, as a first try for the two-loop corrections, in this work, we only consider the ‘‘double scoop’’ diagram (a).

It is very convenient to decompose the expectation values in terms of sub-component Wick contractions. For example, consider the expression $\langle \mathbf{H}_4(\tau_1)\hat{O}(\tau_0)\mathbf{H}_4(\tau_2) \rangle$ in the second line in Eq. (28). It has three types of Wick contractions: $\overbrace{\mathbf{H}_4(\tau_1)\mathbf{H}_4(\tau_2)}$, $\overbrace{\hat{O}(\tau_0)\mathbf{H}_4(\tau_2)}$ and $\overbrace{\mathbf{H}_4(\tau_1)\mathbf{H}_4(\tau_1)}$. Let us define

$$\overbrace{\mathbf{H}_4(\tau_1)\mathbf{H}_4(\tau_2)} \equiv h(\tau_1, \tau_2), \quad \overbrace{\hat{O}(\tau_0)\mathbf{H}_4(\tau_2)} \equiv g(\tau_2), \quad \overbrace{\mathbf{H}_4(\tau_1)\mathbf{H}_4(\tau_1)} \equiv c(\tau_1). \quad (29)$$

With these definitions, considering both terms in the second line of Eq. (28), we obtain,

$$\langle \hat{O}(\tau_0) \rangle = -4 \int_{-\infty}^{\tau_0} d\tau_2 \int_{-\infty}^{\tau_2} d\tau_1 \text{Im}[g(\tau_2)] \text{Im}[c(\tau_1)h(\tau_1, \tau_2)]. \quad (30)$$

Our job is now to calculate the functions $g(\tau_2)$, $c(\tau_1)$ and $h(\tau_1, \tau_2)$ for various possible contractions.

To perform the in-in integrals, we write \mathbf{H}_4 in Eq. (23) as follows (neglecting the non-linear relations between π and \mathcal{R} as discussed before),

$$\mathbf{H}_4 = A_4(\tau) \int d^3\mathbf{x} \mathcal{R}^2 \mathcal{R}'^2 + B_4(\tau) \int d^3\mathbf{x} \mathcal{R}^2 (\partial\mathcal{R})^2, \quad (31)$$

with

$$A_4(\tau) \equiv \frac{1}{2} M_P^2 \eta^2 \epsilon a^2 \left(1 - \frac{h}{\eta^2} \delta(\tau - \tau_e) \tau_e \right), \quad B_4(\tau) \equiv \frac{1}{2} M_P^2 \eta^2 \epsilon a^2 \left(1 + \frac{h}{\eta^2} \delta(\tau - \tau_e) \tau_e \right). \quad (32)$$

In particular, note that the term $\delta(\tau - \tau_e)$ above comes from the term η' in \mathbf{H}_4 as given in Eq. (5).

Depending on which terms in \mathbf{H}_4 are contracted with each other and with $\hat{O}(\tau_0)$, we will have four different contributions as follows:

$$\langle \hat{O}(\tau_0) \rangle = \langle \hat{O} \rangle_{A_4 A_4} + \langle \hat{O} \rangle_{A_4 B_4} + \langle \hat{O} \rangle_{B_4 A_4} + \langle \hat{O} \rangle_{B_4 B_4}, \quad (33)$$

For example, for $\langle \hat{O} \rangle_{A_4 A_4}$ we have

$$\langle \hat{O} \rangle_{A_4 A_4} = \int_{-\infty}^{\tau_0} d\tau_2 \int_{-\infty}^{\tau_2} d\tau_1 A_4(\tau_1) A_4(\tau_2) \int d^3\mathbf{x} \int d^3\mathbf{y} \left\langle \left[\mathcal{R}^2 \mathcal{R}'^2(\mathbf{x}, \tau_1), [\hat{O}(\tau_0), \mathcal{R}^2 \mathcal{R}'^2(\mathbf{y}, \tau_2)] \right] \right\rangle. \quad (34)$$

Going to the Fourier space, this is cast into

$$\begin{aligned} \langle \hat{O} \rangle_{A_4 A_4} = & \int_{-\infty}^{\tau_0} d\tau_2 \int_{-\infty}^{\tau_2} d\tau_1 A_4(\tau_1) A_4(\tau_2) \left[\prod_i^4 \int \frac{d^3\mathbf{q}_i}{(2\pi)^3} (2\pi)^3 \delta^3(\sum_i \mathbf{q}_i) \right] \left[\prod_j^4 \int \frac{d^3\mathbf{k}_j}{(2\pi)^3} (2\pi)^3 \delta^3(\sum_j \mathbf{k}_j) \right] \\ & \times \left\langle \left[(\hat{\mathcal{R}}_{\mathbf{q}_1} \hat{\mathcal{R}}_{\mathbf{q}_2} \hat{\mathcal{R}}'_{\mathbf{q}_3} \hat{\mathcal{R}}'_{\mathbf{q}_4})(\tau_1), \left[(\hat{\mathcal{R}}_{\mathbf{p}_1} \hat{\mathcal{R}}_{\mathbf{p}_2})(\tau_0), (\hat{\mathcal{R}}_{\mathbf{k}_1} \hat{\mathcal{R}}_{\mathbf{k}_2} \hat{\mathcal{R}}'_{\mathbf{k}_3} \hat{\mathcal{R}}'_{\mathbf{k}_4})(\tau_2) \right] \right] \right\rangle. \quad (35) \end{aligned}$$

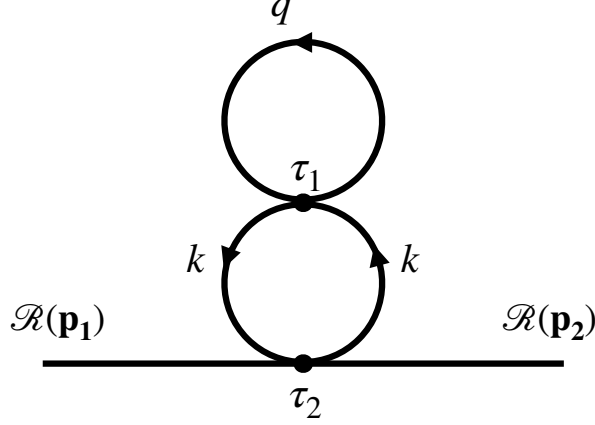


Figure 2: The arrangement of momenta inside each loop and the relative positions of τ_1 and τ_2 .

After performing the contractions and imposing the constraints from the delta functions, in the soft limit where $p \ll q, k$, we end up with the following form of two-loop integrals

$$\langle \mathcal{R}_{\mathbf{p}_1} \mathcal{R}_{\mathbf{p}_2}(\tau_0) \rangle_{A_4 A_4} = (2\pi)^3 \delta^3(\mathbf{p}_1 + \mathbf{p}_2) \int_{-\infty}^{\tau_0} d\tau_2 \int_{-\infty}^{\tau_2} d\tau_1 A_4(\tau_1) A_4(\tau_2) \int \frac{d^3 \mathbf{q}}{(2\pi)^3} \int \frac{d^3 \mathbf{k}}{(2\pi)^3} F(\tau_1, \tau_2; k, q),$$

in which the function $F(\tau_1, \tau_2; k, q)$ is determined by different values of $c(\tau_1)$, $g(\tau_2)$ and $h(\tau_1, \tau_2)$.

There are 9 different terms in $F(\tau_1, \tau_2; k, q)$ from different contractions. We list them as follows,

$$\begin{aligned} (a_0) &: (-4)(2)^2 \text{Im}[\mathcal{R}_p(\tau_0)^2 \mathcal{R}_p^*(\tau_2)^2] \text{Im}[\mathcal{R}'_k(\tau_1)^2 \mathcal{R}'_k^*(\tau_2)^2] |\mathcal{R}_q(\tau_1)|^2 \\ (b_0) &: (-4)(2)^2 \text{Im}[\mathcal{R}_p(\tau_0)^2 \mathcal{R}_p^*(\tau_2)^2] \text{Im}[\mathcal{R}_k(\tau_1)^2 \mathcal{R}'_k^*(\tau_2)^2] |\mathcal{R}'_q(\tau_1)|^2 \\ (c_0) &: (-4)(2)^3 \text{Im}[\mathcal{R}_p(\tau_0)^2 \mathcal{R}_p^*(\tau_2)^2] \text{Im}[\mathcal{R}_k(\tau_1) \mathcal{R}'_k(\tau_1) \mathcal{R}'_k^*(\tau_2)^2] \text{Re}[\mathcal{R}_q(\tau_1) \mathcal{R}'_q(\tau_1)^*], \end{aligned} \quad (36)$$

and

$$\begin{aligned} (d_0) &: (-4)(2)^4 \text{Im}[\mathcal{R}_p(\tau_0)^2 \mathcal{R}_p^*(\tau_2) \mathcal{R}'_p^*(\tau_2)] \text{Im}[\mathcal{R}'_k(\tau_1)^2 \mathcal{R}'_k^*(\tau_2) \mathcal{R}_k^*(\tau_2)] |\mathcal{R}_q(\tau_1)|^2 \\ (e_0) &: (-4)(2)^4 \text{Im}[\mathcal{R}_p(\tau_0)^2 \mathcal{R}_p^*(\tau_2) \mathcal{R}'_p^*(\tau_2)] \text{Im}[\mathcal{R}_k(\tau_1)^2 \mathcal{R}'_k^*(\tau_2) \mathcal{R}_k^*(\tau_2)] |\mathcal{R}'_q(\tau_1)|^2 \\ (f_0) &: (-4)(2)^5 \text{Im}[\mathcal{R}_p(\tau_0)^2 \mathcal{R}_p^*(\tau_2) \mathcal{R}'_p^*(\tau_2)] \text{Im}[\mathcal{R}_k(\tau_1) \mathcal{R}'_k(\tau_1) \mathcal{R}'_k^*(\tau_2) \mathcal{R}_k^*(\tau_2)] \text{Re}[\mathcal{R}_q(\tau_1) \mathcal{R}'_q(\tau_1)^*], \end{aligned} \quad (37)$$

and

$$\begin{aligned} (m) &: (-4)(2)^2 \text{Im}[\mathcal{R}_p(\tau_0)^2 \mathcal{R}'_p^*(\tau_2)^2] \text{Im}[\mathcal{R}'_k(\tau_1)^2 \mathcal{R}'_k^*(\tau_2)^2] |\mathcal{R}_q(\tau_1)|^2, \\ (n) &: (-4)(2)^2 \text{Im}[\mathcal{R}_p(\tau_0)^2 \mathcal{R}'_p^*(\tau_2)^2] \text{Im}[\mathcal{R}_k(\tau_1)^2 \mathcal{R}_k^*(\tau_2)^2] |\mathcal{R}'_q(\tau_1)|^2, \\ (r) &: (-4)(2)^3 \text{Im}[\mathcal{R}_p(\tau_0)^2 \mathcal{R}'_p^*(\tau_2)^2] \text{Im}[\mathcal{R}_k(\tau_1) \mathcal{R}'_k(\tau_1) \mathcal{R}'_k^*(\tau_2)^2] \text{Re}[\mathcal{R}_q(\tau_1) \mathcal{R}'_q(\tau_1)^*]. \end{aligned} \quad (38)$$

One subtle issue in the above expressions is the appearance of the term $\text{Re}[\mathcal{R}_q(\tau_1) \mathcal{R}'_q(\tau_1)^*]$ in terms (c_0) , (f_0) and (r_0) . This term originates from the contraction of $\hat{\mathcal{R}}$ and $\hat{\mathcal{R}}'$ in $\mathcal{R}^2 \mathcal{R}'^2$ in $A_4(\tau_1)$. As $\hat{\mathcal{R}}$ and $\hat{\mathcal{R}}'$ do not commute, we have symmetrized the ordering of $\hat{\mathcal{R}}$ and $\hat{\mathcal{R}}'$ in $A_4(\tau_1)$ which yields to $\text{Re}[\mathcal{R}_q(\tau_1) \mathcal{R}'_q(\tau_1)^*]$ in terms (c_0) , (f_0) and (r) .

Looking at the above expressions we notice that the terms containing momentum q are separated from the terms containing the momentum k . This property is depicted in Fig. 2 where the momentum q runs in the top loop attached to time τ_1 while the momentum k runs in the lower loop attached to both τ_1 and τ_2 . This is a simplifying feature of the diagram (a) in our Feynman diagrams. Because of this separation of the two momenta, it is technically easier to calculate the corrections from diagram (a) compared to diagram (b) in Fig. 1. While this is a simplification, but calculating the time integrals is still a non-trivial task. This is because we have two nested integrals over τ_1 and τ_2 involving 10 factors of $\mathcal{R}(\tau)$ and its derivatives.

The above three classes of contributions in Eqs. (36), (37) and (38) are grouped by their form of the function $c(\tau_1)$ which depends only on the soft momentum p but not on the loop momenta q and k . Now, calculating these common factors in each class, we obtain

$$\text{Im}[\mathcal{R}_p(\tau_0)^2 \mathcal{R}_p^*(\tau_2)^2] = \frac{-H^4 \tau_s^6}{24 M_P^4 \epsilon_i^2 h \tau_e^3 \tau^3 p^3} (h \tau_e^3 + (6-h) \tau^3), \quad (39)$$

$$\text{Im}[\mathcal{R}_p(\tau_0)^2 \mathcal{R}_p^*(\tau_2) \mathcal{R}_p'^*(\tau_2)] = \frac{H^4 \tau_s^6}{16 M_P^4 \epsilon_i^2 \tau^4 p^3}, \quad (40)$$

and

$$\text{Im}[\mathcal{R}_p(\tau_0)^2 \mathcal{R}_p'^*(\tau_2)^2] = \frac{H^4 \tau_s^6 (6 \tau_s^5 - \tau^5)}{40 M_P^4 \epsilon_i^2 \tau^8 p}. \quad (41)$$

Comparing the above three expressions, we conclude that the term in Eq. (41) is much suppressed compared to terms Eq. (39) and Eq. (40) in the soft limit where $p \rightarrow 0$. Correspondingly, we can neglect the contributions of the terms (m), (n) and (r) in Eq. (38).

We present the details of the analysis concerning the remaining three contributions $\langle \hat{O} \rangle_{A_4 B_4}$, $\langle \hat{O} \rangle_{B_4 A_4}$ and $\langle \hat{O} \rangle_{B_4 B_4}$ in the Appendix A.

Before presenting the final result, it is useful to have an estimate of the leading contributions. Let us look at the contributions of terms (a₀) and (b₀). The difference is that in (a₀), \mathcal{R}' comes with k inside the expression $\text{Im}[\mathcal{R}'_k(\tau_1)^2 \mathcal{R}'_k^*(\tau_2)^2]$ while in (b₀), \mathcal{R}' involves the momentum q simply as $|\mathcal{R}'_q(\tau_1)|^2$. On the other hand, for the superhorizon perturbations during the USR phase we have,

$$\mathcal{R}'_q(\tau) \simeq -\frac{3}{\tau} \mathcal{R}_q(\tau) \propto \tau^{-4}. \quad (42)$$

Therefore, the leading effects in the in-in integrals on the superhorizon limit where $\tau_i \rightarrow 0$ are controlled by the contributions of \mathcal{R}' . Since the term (b₀) involves $|\mathcal{R}'_q(\tau_1)|^2$, it scales like τ_1^{-8} while in $\text{Im}[\mathcal{R}'_k(\tau_1)^2 \mathcal{R}'_k^*(\tau_2)^2]$ the dependence can not be steeper than this. Indeed, calculating the leading terms on superhorizon limits of $\tau_1, \tau_2 \rightarrow 0$, one can show that the ratio (a₀)/(b₀) scales like $(k \tau_1)^2$ which becomes smaller than unity on superhorizon scales. Therefore, it is expected that the contribution of term (b₀) to be more dominant than the term (a₀). Indeed, calculating the in-in integrals for both terms (a₀) and (b₀), and neglecting the numerical prefactors and the common $(2\pi)^3 \delta^3(\mathbf{p}_1 + \mathbf{p}_2)$, we obtain that they scale as follows:

$$(a_0) : (\mathcal{P}_{\text{CMB}})^3 e^{12\Delta N} \Delta N, \quad (b_0) : (\mathcal{P}_{\text{CMB}})^3 e^{12\Delta N} \Delta N^2 \quad (43)$$

in which \mathcal{P}_{CMB} is the tree-level CMB scale power spectrum,

$$\mathcal{P}_{\text{CMB}} = \frac{H^2}{8\pi^2\epsilon_i M_P^2}. \quad (44)$$

For large enough ΔN , the contributions from (b_0) is typically larger than that of (a_0) as expected.

As we demonstrated in Appendix A, in total there are 15 leading contributions (i.e. containing p^{-3}) given by $(a_0), (b_0), (c_0), (d_0), (e_0), (f_0), (a_1), (b_1), (c_1), (a_2), (b_2), (c_2), (d_2), (e_2), (f_2), (a_3)$ and (b_3) presented in Appendix A. The contributions from these 15 terms are either like the contribution from the (a_0) term scaling like $e^{12\Delta N}\Delta N$ or like that of the (b_0) term, scaling like $e^{12\Delta N}\Delta N^2$. It turns out that only the contributions from terms $(b_0), (c_0), (d_0), (e_0)$ and (f_0) have the latter form.

In the limit of large enough ΔN , and adding the contributions of terms $(b_0), (c_0), (d_0), (e_0)$ and (f_0) as the leading terms, we obtain the following fractional two-loop correction,

$$\frac{\Delta\mathcal{P}^{(2\text{-loop})}}{\mathcal{P}_{\text{CMB}}} \simeq -\frac{27(23h^2 + 132h + 1152)}{8h} e^{12\Delta N}\Delta N^2\mathcal{P}_{\text{CMB}}^2, \quad (45)$$

where we have neglected the subleading terms involving $\Delta N e^{12\Delta N}$. The fact that the leading two-loop corrections scale like $e^{12\Delta N}\Delta N^2$ is both interesting and reassuring. In addition, the two-loop corrections scale linearly with h for $h \rightarrow -\infty$. Note that our result above is obtained in the limit of sharp enough transition $|h| > 1$ in which the effects of the relaxation during the final SR phase are neglected.

It is instructive to compare the above two-loop corrections associated to diagram **(a)** with the full one-loop correction obtained in [11],

$$\frac{\Delta\mathcal{P}^{(1\text{-loop})}}{\mathcal{P}_{\text{CMB}}} \simeq \frac{6(h^2 + 24h + 180)}{h} e^{6\Delta N}\Delta N\mathcal{P}_{\text{CMB}}. \quad (46)$$

Comparing Eqs. (45) and (46), we obtain

$$\frac{\Delta\mathcal{P}^{(2\text{-loop})}}{\mathcal{P}_{\text{CMB}}} \sim \left(\frac{\Delta\mathcal{P}^{(1\text{-loop})}}{\mathcal{P}_{\text{CMB}}}\right)^2. \quad (47)$$

This is an interesting result, indicating that the fractional two-loop corrections is typically the square of the fractional one-loop correction.

In order for the loop corrections to be under perturbative control, we require that the successive loop corrections to be hierarchical, i.e. $\mathcal{P}_{\text{CMB}} > \Delta\mathcal{P}^{(1\text{-loop})} > \Delta\mathcal{P}^{(2\text{-loop})}$. Neglecting the numerical prefactors, from Eqs. (45) and (46) we obtain,

$$\frac{\Delta\mathcal{P}^{(2\text{-loop})}}{\Delta\mathcal{P}^{(1\text{-loop})}} \sim \frac{\Delta\mathcal{P}^{(1\text{-loop})}}{\mathcal{P}_{\text{CMB}}} \sim e^{6\Delta N}\Delta N\mathcal{P}_{\text{CMB}}. \quad (48)$$

This shows that if the fractional one-loop correction is not small, then the two-loop corrections become significant as well so the perturbative treatment gets quickly out of control. As elaborated in [11], the one-loop correction becomes significant for sharp transition when $|h| \gg 1$ as can be seen in Eq. (46). Therefore, we conclude that the two-loop corrections become significant in model of sharp transition, which can be seen in Eq. (45) too. In order for the loop corrections to be under perturbative control, one has to either have a mild transition with h at the order of slow-roll parameters, or to take the duration of USR phase to be reasonably short, say $\Delta N \lesssim 1$. However,

the latter arrangement may not be suitable for the PBHs formation as we need a long enough period of USR phase to enhance the power spectrum in the first place. For example, with $h = -6$, we need $\Delta N \lesssim 2.3$ to amplify the power spectrum by 7 orders of magnitudes compared to the CMB scale for the purpose of PBHs formation while still satisfying the perturbative bound from one-loop correction in Eq. (46). Therefore, the only safe strategy for PBHs formation in this setup is to employ a mild transition with $|h| \ll 1$.

There are two important comments in order. The first comment is that in this work we studied the corrections from the diagram **(a)** in Fig. 1. Naturally, one may ask how the two-loop corrections from the remaining ten diagram can be compared to the current result given in Eq. (45). In a work in progress [83], we are studying the correction from diagram **(m)** in Fig. 1 involving a single vertex of sextic Hamiltonian. We have confirmed that it scales like Eq. (45). On the physical ground, we expect the full two-loop corrections to have the same general form as in Eq. (45), i.e. scaling like $\Delta N^2 e^{12\Delta N}$. The second comment is the the issue of regularization and renormalization. In the current analysis, we have restricted the momentum in the range $q_s \leq q \leq k_e$. In principle one should integrate over the entire range $q_{IR} < q < q_f$ in which q_{IR} is the lower IR limit while q_f represents the mode which leaves the horizon at the end of inflation. Alternatively, one may simply set $q_f \rightarrow \infty$. While the IR contributions are under control, the UV contribution will diverge which has to be regularized and renormalized. Having said this, the peak of the power spectrum at the end of USR phase and the dimensionless factor $e^{6\Delta N} \mathcal{P}_{\text{CMB}}$ fixes the overall scale of finite term after regularization. The fact that the two-loop corrections in Eq. (45) is the square of the one-loop correction Eq. (46) qualitatively support this expectation. However, it is an important question to study the renormalization of the loop corrections in more detail.

5 Summary and Discussions

In this work, we have looked at the quantum corrections in primordial power spectrum at two-loop orders in models of single field inflation involving an intermediate USR phase employed for PBHs formation. This is the natural continuation of the previous works concerning the one-loop corrections. As the one-loop correction in models with sharp transition to the final SR phase can be large [1, 11], therefore it is necessary to examine the two-loop corrections for the severity of the loop contributions. As we have shown, there are 11 distinct one-particle irreducible Feynman diagrams at the two-loop orders. They require the cubic, quartic, quintic and sextic interaction Hamiltonians.

As a first step forward, we have studied the corrections from the diagram **(a)** in Fig. 1. This is because this diagram involves two vertices of quartic interaction while their momentum integrals over q and k are separable. This brings computational simplicities. Other diagrams in Fig. 1 are more complicated, either having higher order nested integrals or the momentum integrals are not separable. On the other hand, the in-in analysis associated to diagram **(m)** would be easier to handle as it involves a single sextic Hamiltonian vertex. However, one has to calculate the action to sixth order to construct \mathbf{H}_6 which involves additional technical complexities [83]. Our result shows that the two-loop corrections scale as the square of the one-loop corrections, i.e. like $(\Delta N e^{6\Delta N} \mathcal{P}_{\text{CMB}})^2$. This is interesting and physically expected. This result confirms the previous results [1, 11] that the loop corrections can quickly get out of control if the the transition to the final attractor phase is very sharp and the duration of USR phase is long enough. In order for the loop corrections to be

under perturbative control, and at the same time, to generate PBHs with the desired mass scales for dark matter purpose, it is necessary that the transition to the final attractor phase to be mild so the loop corrections are rendered harmless.

There are a few directions in which the current work can be extended. One natural direction to proceed is to consider the loop corrections from the remaining Feynman diagrams in Fig. 1. While this is an interesting and yet cumbersome task, we believe that the total two-loop corrections would be similar to our current result, i.e. scaling like $(\Delta N e^{6\Delta N} \mathcal{P}_{\text{CMB}})^2$. The other direction to investigate is the question of regularization and renormalization at both one-loop and two-loop orders. We would like to come back to this important question in future.

Acknowledgments: We thank Jacopo Fumagalli, Haidar Sheikahmadi, Amin Nassiri-Rad and Bahar Nikbakht for useful discussions. We thank ICCUB, University of Barcelona, for the kind hospitality during the workshop ‘‘BBH initiative: I. Primordial Black Holes’’ where this work was in progress.

A In-In Integrals

In this Appendix we present the in-in analysis in some details.

As explained in the main text, the two-loop corrections have the following contributions,

$$\langle \hat{O}(\tau_0) \rangle = \langle \hat{O} \rangle_{A_4 A_4} + \langle \hat{O} \rangle_{A_4 B_4} + \langle \hat{O} \rangle_{B_4 A_4} + \langle \hat{O} \rangle_{B_4 B_4}. \quad (49)$$

In the main text, we have presented the results for $\langle \hat{O} \rangle_{A_4 A_4}$ which we report here as well for concreteness,

$$\langle \hat{O} \rangle_{A_4 A_4} = \int_{-\infty}^{\tau_0} d\tau_2 \int_{-\infty}^{\tau_2} d\tau_1 A_4(\tau_1) A_4(\tau_2) \int d^3 \mathbf{x} \int d^3 \mathbf{y} \left\langle \left[\mathcal{R}^2 \mathcal{R}'^2(\mathbf{x}, \tau_1), [\hat{O}(\tau_0), \mathcal{R}^2 \mathcal{R}'^2(\mathbf{y}, \tau_2)] \right] \right\rangle. \quad (50)$$

Going to the Fourier space and after performing the contractions and imposing the constraints from the delta functions, in the soft limit where $p \ll q, k$, we obtain

$$\langle \mathcal{R}_{\mathbf{p}_1} \mathcal{R}_{\mathbf{p}_2}(\tau_0) \rangle_{A_4 A_4} = (2\pi)^3 \delta^3(\mathbf{p}_1 + \mathbf{p}_2) \int_{-\infty}^{\tau_0} d\tau_2 \int_{-\infty}^{\tau_2} d\tau_1 A_4(\tau_1) A_4(\tau_2) \int \frac{d^3 \mathbf{q}}{(2\pi)^3} \int \frac{d^3 \mathbf{k}}{(2\pi)^3} F(\tau_1, \tau_2; k, q),$$

in which the function $F(\tau_1, \tau_2; k, q)$ has the following 9 contributions,

$$\begin{aligned} (a_0) &: (-4)(2)^2 \text{Im}[\mathcal{R}_p(\tau_0)^2 \mathcal{R}_p^*(\tau_2)^2] \text{Im}[\mathcal{R}'_k(\tau_1)^2 \mathcal{R}'_k^*(\tau_2)^2] |\mathcal{R}_q(\tau_1)|^2 \\ (b_0) &: (-4)(2)^2 \text{Im}[\mathcal{R}_p(\tau_0)^2 \mathcal{R}_p^*(\tau_2)^2] \text{Im}[\mathcal{R}_k(\tau_1)^2 \mathcal{R}'_k^*(\tau_2)^2] |\mathcal{R}'_q(\tau_1)|^2 \\ (c_0) &: (-4)(2)^3 \text{Im}[\mathcal{R}_p(\tau_0)^2 \mathcal{R}_p^*(\tau_2)^2] \text{Im}[\mathcal{R}_k(\tau_1) \mathcal{R}'_k(\tau_1) \mathcal{R}'_k^*(\tau_2)^2] \text{Re}[\mathcal{R}_q(\tau_1) \mathcal{R}'_q(\tau_1)^*], \end{aligned} \quad (51)$$

and

$$\begin{aligned} (d_0) &: (-4)(2)^4 \text{Im}[\mathcal{R}_p(\tau_0)^2 \mathcal{R}_p^*(\tau_2) \mathcal{R}'_p^*(\tau_2)] \text{Im}[\mathcal{R}'_k(\tau_1)^2 \mathcal{R}'_k^*(\tau_2) \mathcal{R}_k^*(\tau_2)] |\mathcal{R}_q(\tau_1)|^2 \\ (e_0) &: (-4)(2)^4 \text{Im}[\mathcal{R}_p(\tau_0)^2 \mathcal{R}_p^*(\tau_2) \mathcal{R}'_p^*(\tau_2)] \text{Im}[\mathcal{R}_k(\tau_1)^2 \mathcal{R}'_k^*(\tau_2) \mathcal{R}_k^*(\tau_2)] |\mathcal{R}'_q(\tau_1)|^2 \\ (f_0) &: (-4)(2)^5 \text{Im}[\mathcal{R}_p(\tau_0)^2 \mathcal{R}_p^*(\tau_2) \mathcal{R}'_p^*(\tau_2)] \text{Im}[\mathcal{R}_k(\tau_1) \mathcal{R}'_k(\tau_1) \mathcal{R}'_k^*(\tau_2) \mathcal{R}_k^*(\tau_2)] \text{Re}[\mathcal{R}_q(\tau_1) \mathcal{R}'_q(\tau_1)^*], \end{aligned} \quad (52)$$

and

$$\begin{aligned}
(m) &: (-4)(2)^2 \text{Im}[\mathcal{R}_p(\tau_0)^2 \mathcal{R}_p'^*(\tau_2)^2] \text{Im}[\mathcal{R}_k'(\tau_1)^2 \mathcal{R}_k^*(\tau_2)^2] |\mathcal{R}_q(\tau_1)|^2, \\
(n) &: (-4)(2)^2 \text{Im}[\mathcal{R}_p(\tau_0)^2 \mathcal{R}_p'^*(\tau_2)^2] \text{Im}[\mathcal{R}_k(\tau_1)^2 \mathcal{R}_k^*(\tau_2)^2] |\mathcal{R}_q'(\tau_1)|^2, \\
(r) &: (-4)(2)^3 \text{Im}[\mathcal{R}_p(\tau_0)^2 \mathcal{R}_p'^*(\tau_2)^2] \text{Im}[\mathcal{R}_k(\tau_1) \mathcal{R}_k'(\tau_1) \mathcal{R}_k^*(\tau_2)^2] \text{Re}[\mathcal{R}_q(\tau_1) \mathcal{R}_q'(\tau_1)^*]. \quad (53)
\end{aligned}$$

Now we consider the contribution $\langle \hat{O} \rangle_{A_4 B_4}$, yielding

$$\begin{aligned}
\langle \hat{O} \rangle_{A_4 B_4} &= \int_{-\infty}^{\tau_0} d\tau_2 \int_{-\infty}^{\tau_2} d\tau_1 A_4(\tau_1) B_4(\tau_2) \left[\prod_i^4 \int \frac{d^3 \mathbf{q}_i}{(2\pi)^3} (2\pi)^3 \delta^3(\sum_i \mathbf{q}_i) \right] \left[\prod_j^4 \int \frac{d^3 \mathbf{k}_j}{(2\pi)^3} (2\pi)^3 \delta^3(\sum_j \mathbf{k}_j) \right] \\
&\times \left\langle \left[(\hat{\mathcal{R}}_{\mathbf{q}_1} \hat{\mathcal{R}}_{\mathbf{q}_2} \hat{\mathcal{R}}_{\mathbf{q}_3} \hat{\mathcal{R}}_{\mathbf{q}_4})'(\tau_1), \left[(\hat{\mathcal{R}}_{\mathbf{p}_1} \hat{\mathcal{R}}_{\mathbf{p}_2})(\tau_0), (\hat{\mathcal{R}}_{\mathbf{k}_1} \hat{\mathcal{R}}_{\mathbf{k}_2} \hat{\mathcal{R}}_{\mathbf{k}_3} \hat{\mathcal{R}}_{\mathbf{k}_4})(\tau_2) \right] \right] \right\rangle i^2 \mathbf{k}_3 \cdot \mathbf{k}_4. \quad (54)
\end{aligned}$$

The leading contributions are those in which $\hat{\mathcal{R}}_{\mathbf{p}}(\tau_0)$ does not contract with $\hat{\mathcal{R}}_{\mathbf{k}_3}(\tau_2)$ and $\hat{\mathcal{R}}_{\mathbf{k}_4}(\tau_2)$. Correspondingly, the leading terms will be similar to terms (a_0) , (b_0) and (c_0) in the analysis of $\langle \hat{O} \rangle_{A_4 A_4}$. More specifically, the leading terms are,

$$\begin{aligned}
(a_1) &: (-4)(2)^2 \text{Im}[\mathcal{R}_p(\tau_0)^2 \mathcal{R}_p^*(\tau_2)^2] \text{Im}[\mathcal{R}_k'(\tau_1)^2 \mathcal{R}_k^*(\tau_2)^2] |\mathcal{R}_q(\tau_1)|^2 (-i^2 k^2) \\
(b_1) &: (-4)(2)^2 \text{Im}[\mathcal{R}_p(\tau_0)^2 \mathcal{R}_p^*(\tau_2)^2] \text{Im}[\mathcal{R}_k(\tau_1)^2 \mathcal{R}_k^*(\tau_2)^2] |\mathcal{R}_q'(\tau_1)|^2 (-i^2 k^2) \\
(c_1) &: (-4)(2)^3 \text{Im}[\mathcal{R}_p(\tau_0)^2 \mathcal{R}_p^*(\tau_2)^2] \text{Im}[\mathcal{R}_k(\tau_1) \mathcal{R}_k'(\tau_1) \mathcal{R}_k^*(\tau_2)^2] \text{Re}[\mathcal{R}_q(\tau_1) \mathcal{R}_q'(\tau_1)^*] (-i^2 k^2). \quad (55)
\end{aligned}$$

Now consider $\langle \hat{O} \rangle_{B_4 A_4}$, yielding,

$$\begin{aligned}
\langle \hat{O} \rangle_{B_4 A_4} &= \int_{-\infty}^{\tau_0} d\tau_2 \int_{-\infty}^{\tau_2} d\tau_1 B_4(\tau_1) A_4(\tau_2) \left[\prod_i^4 \int \frac{d^3 \mathbf{q}_i}{(2\pi)^3} (2\pi)^3 \delta^3(\sum_i \mathbf{q}_i) \right] \left[\prod_j^4 \int \frac{d^3 \mathbf{k}_j}{(2\pi)^3} (2\pi)^3 \delta^3(\sum_j \mathbf{k}_j) \right] \\
&\times \left\langle \left[(\hat{\mathcal{R}}_{\mathbf{q}_1} \hat{\mathcal{R}}_{\mathbf{q}_2} \hat{\mathcal{R}}_{\mathbf{q}_3} \hat{\mathcal{R}}_{\mathbf{q}_4})(\tau_1), \left[(\hat{\mathcal{R}}_{\mathbf{p}_1} \hat{\mathcal{R}}_{\mathbf{p}_2})(\tau_0), (\hat{\mathcal{R}}_{\mathbf{k}_1} \hat{\mathcal{R}}_{\mathbf{k}_2} \hat{\mathcal{R}}_{\mathbf{k}_3} \hat{\mathcal{R}}_{\mathbf{k}_4})'(\tau_2) \right] \right] \right\rangle i^2 \mathbf{q}_3 \cdot \mathbf{q}_4. \quad (56)
\end{aligned}$$

The leading contributions are like (a_0) , (b_0) , (c_0) , (d_0) , (e_0) and (f_0) in $\langle \hat{O} \rangle_{A_4 A_4}$, yielding

$$\begin{aligned}
(a_2) &: (-4)(2)^2 \text{Im}[\mathcal{R}_p(\tau_0)^2 \mathcal{R}_p^*(\tau_2)^2] \text{Im}[\mathcal{R}_k(\tau_1)^2 \mathcal{R}_k'^*(\tau_2)^2] |\mathcal{R}_q(\tau_1)|^2 (-i^2 k^2) \\
(b_2) &: (-4)(2)^2 \text{Im}[\mathcal{R}_p(\tau_0)^2 \mathcal{R}_p^*(\tau_2)^2] \text{Im}[\mathcal{R}_k(\tau_1)^2 \mathcal{R}_k^*(\tau_2)^2] |\mathcal{R}_q(\tau_1)|^2 (-i^2 q^2) \\
(c_2) &: (-4)(2)^4 \text{Im}[\mathcal{R}_p(\tau_0)^2 \mathcal{R}_p^*(\tau_2)^2] \text{Im}[\mathcal{R}_k(\tau_1)^2 \mathcal{R}_k'^*(\tau_2)^2] |\mathcal{R}_q(\tau_1)|^2 (i^2 \mathbf{k} \cdot \mathbf{q}) \quad (57)
\end{aligned}$$

and

$$\begin{aligned}
(d_2) &: (-4)(2)^4 \text{Im}[\mathcal{R}_p(\tau_0)^2 \mathcal{R}_p^*(\tau_2) \mathcal{R}_p'^*(\tau_2)] \text{Im}[\mathcal{R}_k(\tau_1)^2 \mathcal{R}_k'^*(\tau_2) \mathcal{R}_k^*(\tau_2)] |\mathcal{R}_q(\tau_1)|^2 (-i^2 k^2) \\
(e_2) &: (-4)(2)^4 \text{Im}[\mathcal{R}_p(\tau_0)^2 \mathcal{R}_p^*(\tau_2) \mathcal{R}_p'^*(\tau_2)] \text{Im}[\mathcal{R}_k(\tau_1)^2 \mathcal{R}_k'^*(\tau_2) \mathcal{R}_k^*(\tau_2)] |\mathcal{R}_q(\tau_1)|^2 (-i^2 q^2) \\
(f_2) &: (-4)(2)^6 \text{Im}[\mathcal{R}_p(\tau_0)^2 \mathcal{R}_p^*(\tau_2) \mathcal{R}_p'^*(\tau_2)] \text{Im}[\mathcal{R}_k(\tau_1)^2 \mathcal{R}_k'^*(\tau_2) \mathcal{R}_k^*(\tau_2)] |\mathcal{R}_q(\tau_1)|^2 (i^2 \mathbf{k} \cdot \mathbf{q}) \quad (58)
\end{aligned}$$

From the 6 terms above, one can check that the terms (c_2) and (f_2) make zero contributions after performing the double momentum integrals of the form $\int d^3 \mathbf{q} d^3 \mathbf{k} (\mathbf{q} \cdot \mathbf{k}) \mathcal{F}(\tau_1, \tau_2; k, q)$ which vanishes.

Finally, considering $\langle \hat{O} \rangle_{B_4 B_4}$, we have

$$\begin{aligned} \langle \hat{O} \rangle_{B_4 B_4} &= \int_{-\infty}^{\tau_0} d\tau_2 \int_{-\infty}^{\tau_2} d\tau_1 B_4(\tau_1) B_4(\tau_2) \left[\prod_i^4 \int \frac{d^3 \mathbf{q}_i}{(2\pi)^3} (2\pi)^3 \delta^3(\sum_i \mathbf{q}_i) \right] \left[\prod_j^4 \int \frac{d^3 \mathbf{k}_j}{(2\pi)^3} (2\pi)^3 \delta^3(\sum_j \mathbf{k}_j) \right] \\ &\times \left\langle \left[(\hat{\mathcal{R}}_{\mathbf{q}_1} \hat{\mathcal{R}}_{\mathbf{q}_2} \hat{\mathcal{R}}_{\mathbf{q}_3} \hat{\mathcal{R}}_{\mathbf{q}_4})(\tau_1), \left[(\hat{\mathcal{R}}_{\mathbf{p}_1} \hat{\mathcal{R}}_{\mathbf{p}_2})(\tau_0), (\hat{\mathcal{R}}_{\mathbf{k}_1} \hat{\mathcal{R}}_{\mathbf{k}_2} \hat{\mathcal{R}}_{\mathbf{k}_3} \hat{\mathcal{R}}_{\mathbf{k}_4})(\tau_2) \right] \right] \right\rangle (\mathbf{q}_3 \cdot \mathbf{q}_4) (\mathbf{k}_3 \cdot \mathbf{k}_4). \end{aligned} \quad (59)$$

The leading contributions are like (a_0) and (b_0) terms, yielding

$$\begin{aligned} (a_3) &: (-4)(2)^2 \text{Im}[\mathcal{R}_p(\tau_0)^2 \mathcal{R}_p^*(\tau_2)^2] \text{Im}[\mathcal{R}_k(\tau_1)^2 \mathcal{R}_k^*(\tau_2)^2] |\mathcal{R}_q(\tau_1)|^2 (-i^2 k^2)^2 \\ (b_3) &: (-4)(2)^2 \text{Im}[\mathcal{R}_p(\tau_0)^2 \mathcal{R}_p^*(\tau_2)^2] \text{Im}[\mathcal{R}_k(\tau_1)^2 \mathcal{R}_k^*(\tau_2)^2] |\mathcal{R}_q(\tau_1)|^2 (-i^2 k^2) (-i^2 q^2) \end{aligned} \quad (60)$$

So in total, we have 15 leading terms (i.e. containing p^{-3}) given by $(a_0), (b_0), (c_0), (d_0), (e_0), (f_0), (a_1), (b_1), (c_1), (a_2), (b_2), (c_2), (d_2), (e_2), (f_2), (a_3)$ and (b_3) listed above. Out of these 15 contributions, only the terms $(b_0), (c_0), (d_0), (e_0), (f_0)$ scale like $\Delta N^2 e^{12\Delta N}$ while the remaining terms scale like $\Delta N e^{12\Delta N}$. In the limit of large enough ΔN , we may neglect the latter contributions as the subleading corrections.

Calculating the leading terms from $(b_0), (c_0), (d_0), (e_0), (f_0)$, and neglecting the common factor $(2\pi)^3 \delta^3(\mathbf{p}_1 + \mathbf{p}_2)$ and $\frac{(4\pi)^2}{(2\pi)^6}$ from the double azimuthal integrals over momentum, we obtain,

$$(b_0) : \frac{27H^6}{512M_P^6 \epsilon_i^3 h p^3} (h^2 + 28h - 384) \Delta N^2 e^{12\Delta N} + \mathcal{O}(\Delta N), \quad (61)$$

$$(c_0) : \frac{-27H^6}{64M_P^6 \epsilon_i^3 h p^3} (h^2 + 8h + 96) \Delta N^2 e^{12\Delta N} + \mathcal{O}(\Delta N), \quad (62)$$

$$(d_0) : \frac{9H^6}{256M_P^6 \epsilon_i^3 h p^3} (h^2 + 8h + 48) \Delta N^2 e^{12\Delta N} + \mathcal{O}(\Delta N), \quad (63)$$

$$(e_0) : \frac{-9H^6}{256M_P^6 \epsilon_i^3 h p^3} (h^2 + 16h + 96) \Delta N^2 e^{12\Delta N} + \mathcal{O}(\Delta N), \quad (64)$$

$$(f_0) : \frac{-9H^6}{16M_P^6 \epsilon_i^3 h p^3} (h + 6) \Delta N^2 e^{12\Delta N} + \mathcal{O}(\Delta N). \quad (65)$$

Combining the above five contributions, and including all numerical factors, we obtain our final result,

$$\langle \mathcal{R}_{\mathbf{p}_1} \mathcal{R}_{\mathbf{p}_2} \rangle \Big|_{2\text{-loops}} = (2\pi)^3 \delta^3(\mathbf{p}_1 + \mathbf{p}_2) \frac{-27H^6 (4\pi)^2}{512M_P^6 \epsilon_i^3 h p^3 (2\pi)^6} (23h^2 + 132h + 1152) \Delta N^2 e^{12\Delta N} + \mathcal{O}(\Delta N).$$

Now, multiplying by the factor $\frac{p^3}{2\pi^2}$ to construct the dimensionless power spectrum, we end up with our fractional two-loop correction as follows,

$$\frac{\Delta \mathcal{P}^{(2\text{-loop})}}{\mathcal{P}_{\text{CMB}}} \simeq -\frac{27(23h^2 + 132h + 1152)}{8h} e^{12\Delta N} N^2 \mathcal{P}_{\text{CMB}}^2 + \mathcal{O}(\Delta N), \quad (66)$$

where \mathcal{P}_{CMB} is the tree-level power spectrum for the CMB scale modes given in Eq. (44).

References

- [1] J. Kristiano and J. Yokoyama, Phys. Rev. Lett. **132**, no.22, 221003 (2024), [arXiv:2211.03395 [hep-th]].
- [2] J. Kristiano and J. Yokoyama, Phys. Rev. D **109**, no.10, 103541 (2024), [arXiv:2303.00341 [hep-th]].
- [3] A. Riotto, [arXiv:2301.00599 [astro-ph.CO]].
- [4] A. Riotto, [arXiv:2303.01727 [astro-ph.CO]].
- [5] S. Choudhury, M. R. Gangopadhyay and M. Sami, Eur. Phys. J. C **84**, no.9, 884 (2024), [arXiv:2301.10000 [astro-ph.CO]].
- [6] S. Choudhury, S. Panda and M. Sami, Phys. Lett. B **845**, 138123 (2023), [arXiv:2302.05655 [astro-ph.CO]].
- [7] S. Choudhury, S. Panda and M. Sami, JCAP **11**, 066 (2023), [arXiv:2303.06066 [astro-ph.CO]].
- [8] S. Choudhury, S. Panda and M. Sami, JCAP **08**, 078 (2023), [arXiv:2304.04065 [astro-ph.CO]].
- [9] S. Choudhury, A. Karde, S. Panda and M. Sami, JCAP **07**, 034 (2024), [arXiv:2401.10925 [astro-ph.CO]].
- [10] S. Choudhury and M. Sami, [arXiv:2407.17006 [gr-qc]].
- [11] H. Firouzjahi, JCAP **10**, 006 (2023), [arXiv:2303.12025 [astro-ph.CO]].
- [12] H. Motohashi and Y. Tada, JCAP **08**, 069 (2023), [arXiv:2303.16035 [astro-ph.CO]].
- [13] H. Firouzjahi and A. Riotto, JCAP **02**, 021 (2024), [arXiv:2304.07801 [astro-ph.CO]].
- [14] G. Tasinato, Phys. Rev. D **108**, no.4, 043526 (2023), [arXiv:2305.11568 [hep-th]].
- [15] G. Franciolini, A. Iovino, Junior., M. Taoso and A. Urbano, Phys. Rev. D **109**, no.12, 123550 (2024), [arXiv:2305.03491 [astro-ph.CO]].
- [16] H. Firouzjahi, Phys. Rev. D **108**, no.4, 043532 (2023), [arXiv:2305.01527 [astro-ph.CO]].
- [17] S. Maity, H. V. Ragavendra, S. K. Sethi and L. Sriramkumar, JCAP **05**, 046 (2024), [arXiv:2307.13636 [astro-ph.CO]].
- [18] S. L. Cheng, D. S. Lee and K. W. Ng, JCAP **03**, 008 (2024), [arXiv:2305.16810 [astro-ph.CO]].
- [19] J. Fumagalli, S. Bhattacharya, M. Peloso, S. Renaux-Petel and L. T. Witkowski, JCAP **04**, 029 (2024), [arXiv:2307.08358 [astro-ph.CO]].
- [20] A. Nassiri-Rad and K. Asadi, JCAP **04**, 009 (2024), [arXiv:2310.11427 [astro-ph.CO]].
- [21] D. S. Meng, C. Yuan and Q. g. Huang, Phys. Rev. D **106**, no.6, 063508 (2022).
- [22] S. L. Cheng, D. S. Lee and K. W. Ng, Phys. Lett. B **827**, 136956 (2022).

- [23] J. Fumagalli, [arXiv:2305.19263 [astro-ph.CO]].
- [24] Y. Tada, T. Terada and J. Tokuda, *JHEP* **01**, 105 (2024), [arXiv:2308.04732 [hep-th]].
- [25] H. Firouzjahi, *Phys. Rev. D* **109**, no.4, 043514 (2024), [arXiv:2311.04080 [astro-ph.CO]].
- [26] L. Iacconi and D. J. Mulryne, *JCAP* **09**, 033 (2023).
- [27] M. W. Davies, L. Iacconi and D. J. Mulryne, *JCAP* **04**, 050 (2024), [arXiv:2312.05694 [astro-ph.CO]].
- [28] L. Iacconi, D. Mulryne and D. Seery, *JCAP* **06**, 062 (2024), [arXiv:2312.12424 [astro-ph.CO]].
- [29] J. Kristiano and J. Yokoyama, *JCAP* **10**, 036 (2024), [arXiv:2405.12145 [astro-ph.CO]].
- [30] J. Kristiano and J. Yokoyama, [arXiv:2405.12149 [astro-ph.CO]].
- [31] G. Ballesteros and J. G. Egea, *JCAP* **07**, 052 (2024), [arXiv:2404.07196 [astro-ph.CO]].
- [32] R. Kawaguchi, S. Tsujikawa and Y. Yamada, *Phys. Lett. B* **856**, 138962 (2024), [arXiv:2403.16022 [hep-th]].
- [33] M. Braglia and L. Pinol, *JHEP* **08**, 068 (2024), [arXiv:2403.14558 [astro-ph.CO]].
- [34] H. Firouzjahi, *Phys. Rev. D* **110**, no.4, 043519 (2024), [arXiv:2403.03841 [astro-ph.CO]].
- [35] A. Caravano, G. Franciolini and S. Renaux-Petel, [arXiv:2410.23942 [astro-ph.CO]].
- [36] S. Saburov and S. V. Ketov, *Universe* **10**, no.9, 354 (2024), [arXiv:2402.02934 [gr-qc]].
- [37] D. Seery, *JCAP* **02**, 006 (2008), [arXiv:0707.3378 [astro-ph]].
- [38] D. Seery, *JCAP* **11**, 025 (2007), [arXiv:0707.3377 [astro-ph]].
- [39] L. Senatore and M. Zaldarriaga, *JHEP* **12**, 008 (2010), [arXiv:0912.2734 [hep-th]].
- [40] G. L. Pimentel, L. Senatore and M. Zaldarriaga, *JHEP* **07**, 166 (2012).
- [41] K. Inomata, M. Braglia, X. Chen and S. Renaux-Petel, *JCAP* **04**, 011 (2023), [erratum: *JCAP* **09**, E01 (2023)], [arXiv:2211.02586 [astro-ph.CO]].
- [42] P. Ivanov, P. Naselsky and I. Novikov, *Phys. Rev. D* **50**, 7173-7178 (1994).
- [43] J. Garcia-Bellido and E. Ruiz Morales, *Phys. Dark Univ.* **18**, 47-54 (2017).
- [44] C. Germani and T. Prokopec, *Phys. Dark Univ.* **18**, 6-10 (2017).
- [45] M. Biagetti, G. Franciolini, A. Kehagias and A. Riotto, *JCAP* **07**, 032 (2018).
- [46] M. Y. Khlopov, *Res. Astron. Astrophys.* **10**, 495-528 (2010), [arXiv:0801.0116 [astro-ph]].
- [47] O. Özsoy and G. Tasinato, *Universe* **9**, no.5, 203 (2023), [arXiv:2301.03600 [astro-ph.CO]].
- [48] C. T. Byrnes and P. S. Cole, [arXiv:2112.05716 [astro-ph.CO]].

- [49] A. Escrivà, F. Kuhnel and Y. Tada, [arXiv:2211.05767 [astro-ph.CO]].
- [50] S. Pi, [arXiv:2404.06151 [astro-ph.CO]].
- [51] J. M. Maldacena, JHEP **0305**, 013 (2003), [astro-ph/0210603].
- [52] P. R. Jarnhus and M. S. Sloth, JCAP **02**, 013 (2008), [arXiv:0709.2708 [hep-th]].
- [53] F. Arroja and K. Koyama, Phys. Rev. D **77**, 083517 (2008), [arXiv:0802.1167 [hep-th]].
- [54] K. Inomata, Phys. Rev. Lett. **133**, no.14, 141001 (2024), [arXiv:2403.04682 [astro-ph.CO]].
- [55] R. Kawaguchi, S. Tsujikawa and Y. Yamada, [arXiv:2407.19742 [hep-th]].
- [56] J. Fumagalli, [arXiv:2408.08296 [astro-ph.CO]].
- [57] W. H. Kinney, Phys. Rev. D **72**, 023515 (2005), [gr-qc/0503017].
- [58] M. H. Namjoo, H. Firouzjahi and M. Sasaki, Europhys. Lett. **101**, 39001 (2013).
- [59] J. Martin, H. Motohashi and T. Suyama, Phys. Rev. D **87**, no.2, 023514 (2013).
- [60] X. Chen, H. Firouzjahi, M. H. Namjoo and M. Sasaki, Europhys. Lett. **102**, 59001 (2013).
- [61] M. J. P. Morse and W. H. Kinney, Phys. Rev. D **97**, no.12, 123519 (2018).
- [62] W. C. Lin, M. J. P. Morse and W. H. Kinney, JCAP **09**, 063 (2019).
- [63] K. Dimopoulos, Phys. Lett. B **775**, 262-265 (2017), [arXiv:1707.05644 [hep-ph]].
- [64] X. Chen, H. Firouzjahi, E. Komatsu, M. H. Namjoo and M. Sasaki, JCAP **1312**, 039 (2013).
- [65] M. Akhshik, H. Firouzjahi and S. Jazayeri, JCAP **07**, 048 (2015), [arXiv:1501.01099 [hep-th]].
- [66] M. Akhshik, H. Firouzjahi and S. Jazayeri, JCAP **12**, 027 (2015), [arXiv:1508.03293 [hep-th]].
- [67] S. Mooij and G. A. Palma, JCAP **11**, 025 (2015), [arXiv:1502.03458 [astro-ph.CO]].
- [68] R. Bravo, S. Mooij, G. A. Palma and B. Pradenas, JCAP **05**, 024 (2018).
- [69] B. Finelli, G. Goon, E. Pajer and L. Santoni, Phys. Rev. D **97**, no.6, 063531 (2018).
- [70] S. Passaglia, W. Hu and H. Motohashi, Phys. Rev. D **99**, no.4, 043536 (2019).
- [71] S. Pi and M. Sasaki, Phys. Rev. Lett. **131**, no.1, 011002 (2023).
- [72] O. Özsoy and G. Tasinato, Phys. Rev. D **105**, no.2, 023524 (2022),
- [73] H. Firouzjahi and A. Riotto, Phys. Rev. D **108**, no.12, 123504 (2023).
- [74] M. H. Namjoo, JCAP **05**, 041 (2024), [arXiv:2311.12777 [astro-ph.CO]].
- [75] M. H. Namjoo and B. Nikbakht, JCAP **08**, 005 (2024), [arXiv:2401.12958 [astro-ph.CO]].
- [76] Y. F. Cai, X. Chen, M. H. Namjoo, M. Sasaki, D. G. Wang and Z. Wang, JCAP **05**, 012 (2018).

- [77] C. Cheung, P. Creminelli, A. L. Fitzpatrick, J. Kaplan and L. Senatore, JHEP **0803**, 014 (2008).
- [78] C. Cheung, A. L. Fitzpatrick, J. Kaplan and L. Senatore, JCAP **0802**, 021 (2008).
- [79] S. Weinberg, Phys. Rev. D **72**, 043514 (2005) . [arXiv:hep-th/0506236 [hep-th]].
- [80] X. Chen, M. x. Huang and G. Shiu, Phys. Rev. D **74**, 121301 (2006).
- [81] X. Chen, B. Hu, M. x. Huang, G. Shiu and Y. Wang, JCAP **08**, 008 (2009).
- [82] S. Weinberg, “The Quantum theory of fields. Vol. 1: Foundations,” Cambridge University Press, 2005.
- [83] Hassan Firouzjahi and Bahar Nikbakht, work in progress.